Indian J Med Res 152, September 2020, pp 244-253
DOI: 10.4103/ijmr.IJMR_1823_18

Quick Response Code:

Study of long non-coding RNA highly upregulated in liver cancer (HULC) in breast cancer: A clinical & *in vitro* investigation

Reyhaneh Ravanbakhsh Gavgani[1], Esmaeil Babaei[1], Mohammad Ali Hosseinpourfeizi[1], Ashraf Fakhrjou[2] & Vahid Montazeri[3]

[1]Department of Animal Biology, School of Natural Sciences, University of Tabriz, [2]Department of Pathology, Faculty of Medicine, Tabriz University of Medical Sciences & [3]Department of Thoracic Surgery, Noor-Nejat Hospital, Tabriz, Iran

Received October 1, 2018

***Background & objectives*: Breast cancer remains the most common malignancy among women worldwide. Long non-coding RNAs (lncRNAs) have been shown to play critical roles in tumour initiation and progression. This study was aimed to evaluate the potential role of lncRNA highly upregulated in liver cancer (HULC) in breast cancer.**

***Methods*: The expression of *HULC* was evaluated in breast cancer patients and cell lines using real-time quantitative reverse transcription polymerase chain reaction. Small interfering RNA-based knockdown was also employed to study the potential role of *HULC* in breast cancer cell lines including ZR-75-1, MCF7 and MDA-MB-231.**

***Results*: *HULC* was significantly upregulated in tumour tissues compared to non-tumoural margins (P<0.001). The receiver operating characteristic (ROC) curve analysis demonstrated the biomarker potential of *HULC* (ROC^{AUC}=0.78, P<0.001). The *HULC* knockdown induced apoptosis and suppressed cellular migration in breast cancer cell lines.**

***Interpretation & conclusions*: Our results indicated that *HULC* was upregulated in breast cancer and might play a role in tumourigenesis. The *HULC* may have a potential to be exploited as a new biomarker and therapeutic target in breast cancer.**

Key words Biomarker - breast cancer - HULC - long non-coding RNA - small interfering RNA

Breast cancer is the most common malignancy and the second leading cause of death in women worldwide[1]. This is classified according to molecular subtype into the four main groups in which triple-negative subtypes are more often highly invasive, spreading to lymph nodes while primary tumours are small and leading to early relapse with increased risk of visceral metastasis and poor outcome[2]. Applying genetic biomarkers could be one of the diagnostic and/or prognostic criteria in this area. Therefore, understanding the molecular and genetic networks that control the initiation, progression and spread of cancer

will be useful for finding potential biomarkers. The transcriptome sequencing technologies have revealed that around 90 per cent of the human genome is actively transcribed into non-coding RNAs (ncRNAs), while nearly 20,000 genes, accounting for less than two per cent of the genome, encode proteins[3].

Long ncRNAs (lncRNAs) are endogenous cellular RNA molecules longer than 200 nucleotides in length[4]. Emerging evidence indicates that lncRNAs play an important role in various cell pathways, including proliferation and apoptosis[5,6], autophagy[7], epigenetics[8], invasion and metastasis[9] and lipid metabolism[10]. Aberrant expression of lncRNAs may cause adverse effects on biological processes and lead to many diseases particularly different kinds of cancers including glioma[11], osteosarcoma[12], lung cancer[13] and hepatocellular carcinoma (HCC)[14].

Highly upregulated in liver cancer (*HULC*) gene was reported for the first time as the most overexpressed lncRNA in patients with HCC[15], and also its potential as a diagnostic biomarker has been proposed[16,17]. LncRNA *HULC* with two exons, but no protein-coding function is located on chromosome 6p24.3. Cumulating evidence has shown that *HULC* is not HCC-specific lncRNA, but it is also involved in other cancers such as gastric[7] and glioma[11]. However, there are no data on the potential role of *HULC* in breast cancer.

Therefore, this study was aimed to detect and evaluate the expression level of *HULC* in breast invasive ductal carcinoma and its role as a potential biomarker.

Material & Methods

Human tissue specimens: Fifty two specimens of surgically resected breast tumours with invasive ductal carcinoma subtype and their adjacent non-tumour tissues were collected from Emam Reza and Noor-Nejat hospitals, Tabriz, Iran, from women of age range, 34-80 (51.29±1.73) years. Written informed consent was obtained from all patients prior to sample collection and also, this study was carried out with the approval of the Ethics Committee of the Tabriz University of Medical Sciences (approval number: IR.TBZMED.REC.1392.249), during September 2014 till March 2018. The specimens were immediately frozen in liquid nitrogen after surgery and stored at −80°C until RNA extraction. To classify the tumours, the tumour, node and metastasis (TNM) staging was done according to the American Joint Committee on Cancer[18].

Cell culture: All human breast cancer cell lines including ZR-75-1 (ATCC No. CRL-1500), MCF-7 (ATCC No. HTB-22), MDA-MB-231 (ATCC No. HTB-26) and SkBr-3 (ATCC No. HTB-30) were obtained from the cell bank of Pasteur Institute (Tehran, Iran). ZR-75-1, MCF-7 and SkBr-3 cells were cultured in RPMI-1640 (Roswell Park Memorial Institute-1640) (Gibco, Life Technologies, USA), while MDA-MB-231 was grown in DMEM (Dulbecco's Modified Eagle's Medium) (Sigma-Aldrich, USA) supplemented with 10 per cent heat-inactivated FBS (foetal bovine serum) (Gibco, USA) and 100 U/ml of penicillin/streptomycin (10,000 U/ml, Gibco, USA) at 37°C in a humidified environment containing five per cent CO_2.

RNA extraction, cDNA synthesis and real-time quantitative reverse transcription PCR (qRT-PCR): Total RNA was extracted using TRIzol reagent (Invitrogen, USA) according to the manufacturer's instructions. cDNA (complementary DNA) was synthesized by reverse transcription of 1 µg of total RNA using the PrimeScript RT kit (Takara, China) by following the manufacturer's protocol. The real-time qRT-PCR was carried out with primers specific for *HULC*, *Bax*, *Bcl-2*, *CDH1*, *VIM*, *MMP-9* and *β-actin* using SYBR® Premix EX TaqTM II (Tli RNaseH Plus, Takara, PR China) by Corbett Rotor-Gene 6000 (Corbett Life Sciences, Germany). Primer sequences and real-time qRT-PCR conditions have been outlined in Table I. *β-actin* served as an endogenous control for normalization. The identity of *HULC* gene after being amplified in PCR was further confirmed by sequencing.

Small interfering RNA (siRNA) transfection: To investigate the role of *HULC*, its expression was suppressed through siRNA-mediated gene knockdown. Therefore, pre-designed negative control scrambled siRNA (si-NC) was purchased from Dharmacon (Lafayette, USA) and pre-designed si-*HULC*, against *HULC*, (target sequence: 5'-GGCCGGAATATTCTTTGTTTA-3') was purchased by Qiagen, Germany. Both siRNAs were labelled with 6-FAM (6-carboxyfluorescein) at their 3' end and transfected into cells using HiPerFect Transfection Reagent (Qiagen, Germany) according to the manufacturer's protocol. Assays were conducted 72 h after transfection.

Study of apoptosis: To determine apoptosis, acridine orange/ethidium bromide (AO/EtBr) staining was done. Breast cancer cell lines, including MCF-7 (1.5×10^5),

Table I. Sequences of primers used and their real-time qRT-PCR programmes

Genes	Primer sequence (5'-3')	Real-time qRT-PCR programme[#]	Product size (bp)
HULC	F: ATCGTGGACATTTCAACCTC R: GCTGTGCTTAGTTTATTGCC	D: 95°C for 25 sec A: 59°C for 25 sec E: 72°C for 25 sec	161
Bax	F: GCAAACTGGTGCTCAAGG R: ACTCCCGCCACAAAGA	D: 95°C for 30 sec A: 63°C for 35 sec E: 72°C for 30 sec	236
Bcl-2	F: TGGGAAGTTTCAAATCAGC R: GCATTCTTGGACGAGGG	D: 95°C for 25 sec A: 63°C for 30 sec E: 72°C for 30 sec	298
CDH1	F: AGTACAACGACCCAACCCAAG R: GCAAGAATTCCTCCAAGAATCC	D: 95°C for 30 sec A: 57°C for 22 sec E: 72°C for 20 sec	235
VIM	F: CAGGCAAAGCAGGAGTCCA R: AAGTTCTCTTCCATTTCACGCA	D: 95°C for 30 sec A: 59°C for 35 sec E: 72°C for 30 sec	122
MMP-9	F: CCGCTCACCTTCACTCGC R: ACCACAACTCGTCATCGTC	D: 95°C for 30 sec A: 63°C for 35 sec E: 72°C for 30 sec	174
β-actin	F: AGAGCTACGAGCTGCCTGAC R: AGCACTGTGTTGGCGTACAG	D: 95°C for 30 sec A: 59°C for 30 sec E: 72°C for 30 sec	184

[#]real-time qRT-PCR cycling was started for all primers with initial denaturation at 95°C for 10 minutes. D, denaturation; A, primer annealing, E, extension; real-time qRT-PCR, real-time quantitative reverse transcription polymerase chain reaction; F, forward; R, reverse

MDA-MB-231 (1×10^5) and ZR-75-1 (2.5×10^5), were seeded into 24-well plates (MatTek, USA) and cultured for 24 h, followed by transfection with si-*HULC* and si-NC separately according to the manufacturer's instructions (Qiagen, Germany and Dharmacon, USA, respectively). After 72 h, the cells were collected by traditional trypsin-ethylenediaminetetraacetic acid (EDTA) (0.25%; HyClone, GE Healthcare Life Sciences) treatment and transferred onto glass microscope slides followed by staining with AO/EtBr. Finally, the cells were analyzed under a fluorescence microscope (Olympus BX 41, Germany). Expression levels of genes involved in apoptosis such as *Bax* and *Bcl-2* were also evaluated by real-time qRT-PCR alongside morphological evaluation of the apoptotic cells.

Cell cycle analysis: For cell cycle analysis, MCF-7 (1.5×10^5), MDA-MB-231 (1×10^5) and ZR-75-1 (2.5×10^5) cell lines were seeded into 24-well plates for 24 h. The cells were transfected with si-*HULC* and si-NC separately according to the manufacturer's instruction (Qiagen, Germany and Dharmacon, USA, respectively). After 72 h, the cells were detached by trypsin-EDTA solution at 37°C for five minutes (MCF-7 and ZR-75-1) and two minutes (MDA-MB-231), followed by inhibiting trypsin activity by adding 10 per cent FBS. Afterwards, the cells were collected by traditional trypsin-EDTA treatment and washed by cold phosphate-buffered saline (PBS), *p*H 7.4, followed by fixation using ice-cold ethanol (70% w/w). The cells were incubated in a freshly prepared solution containing 0.1 per cent Triton X-100, RNase A (50 µg/ml; Fermentas, USA), and propidium iodide (PI) (50 µg/ml; Sigma-Aldrich, USA) at 4 °C for 15 minutes. The stained cells were analyzed by flow cytometry (BD FACS Calibur flow cytometer, BD Biosciences, USA). The percentages of measured cells in the sub-G1 and G1 phases were analyzed by FlowJO 7.6.1 software (BD, USA). The experiments were conducted three times independently.

Wound healing assay: In order to get around 90 per cent confluency after 24 h of culturing, each cell line was seeded at appropriate numbers into 24-well plates in complete medium (Gibco, Life Technologies, USA).

After 24 h, a single wound was created in the middle of the well using a sterile 200 µl pipette tip. After removing detached cells with PBS, each cell line was separately transfected by si-*HULC* and si-NC according to the manufacturer's protocol (Qiagen, Germany and Dharmacon, USA, respectively). After 72 h, the cells migrated into the wound area were photographed under the inverted microscope (Olympus, Japan). Beside wound healing assay, the expression of some genes involved in invasion and metastasis including *CDH1* (E-cadherin), *VIM* (vimentin) and *MMP-9* (matrix metallopeptidase-9) was also evaluated at mRNA levels. Since vimentin is usually undetectable in MCF-7 and ZR-75-1, and E-cadherin is below the detection limit in MDA-MB-231, *CDH1* and *MMP-9* expression were evaluated at mRNA levels in ZR-75-1 and MCF-7 and *VIM* and *MMP-9* in MDA-MB-231.

Statistical analysis: Relative Expression Software Tool (REST) 2009 (Corbett Research, Sydney, Australia), was used to evaluate the expression of *HULC* in breast cancer tissues compared to non-tumoural counterparts. The fold change and relative expression levels of studied genes in treated versus non-treated cells were calculated by the $2^{-\Delta\Delta Ct}$ and $2^{-\Delta Ct}$ methods[19], respectively. In these methods, ΔCt=Ct (*HULC*) – Ct (*β-actin*) and ΔΔCt=ΔCt (treated cells) – ΔCt (control), where Ct is cycle threshold. Statistical analysis between two groups was performed by Student's t test and for more than two groups; one-way analysis of variance (one-way ANOVA) was applied. Data were analyzed by SPSS software v22.0 (IBM, Armonk, NY, USA). To assess the biomarker potential of *HULC* in breast cancer a receiver operating characteristic (ROC) curve was drawn using SigmaPlot software v12.5 (Systat Software Inc., USA). All experiments were repeated three times, and data were represented as mean±standard error of mean.

Results

HULC overexpressed in breast cancer tissues: Our preliminary data showed that *HULC* was expressed in breast tumour tissues (Fig. 1A and B) and fold change expressions of *HULC* at mRNA levels calculated through REST, were significantly upregulated by 8.26-fold in cancerous tissues compared to non-cancerous specimens (8.258±0.726, $P<0.001$) (Fig. 1B). The high expression of *HULC* was significantly associated with advanced clinical stages of studied samples ($P=0.025$). Moreover, a marginal association was observed between elevated expression of *HULC* and lymph node metastasis ($P=0.052$) and high oestrogen receptor expression ($P=0.088$) (Table II). No association between expression of *HULC* and other clinicopathological characteristics, including age, differentiation, progesterone and HER-2 expression levels and tumour location, were found (Table II). ROC curve analysis was employed to determine whether or not tumour and non-tumour tissue could be distinguished by the expression level of *HULC*. Pair-matched adjacent normal tissues were used as a control to plot ROC curve. The area under the ROC curve (AUC) was 0.78 ($P<0.001$) indicating its potential as a biomarker (Fig. 1C). The sensitivity and specificity were 0.71 and 0.77, respectively, and the cut-off value was 17.1.

Expression of HULC in breast cancer cell lines: To further explore the potential role of *HULC* in breast cancer, siRNA-based knockdown was employed in ZR-75-1, MCF-7 and MDA-MB-231 cell lines. Data for expression of *HULC* in breast cancer cell lines have been illustrated in Figure 2A. Real-time qRT-PCR analysis of *HULC* expression levels was performed 72 h after transfection indicating knockdown efficiency >70 per cent for all cell lines (Fold reduction in *HULC* expression was significant ($P< 0.05$ & <0.01) (Fig. 2B).

HULC silencing induces apoptosis in breast cancer cell lines: To study apoptosis, treated and non-treated cells were stained with AO/EtBr, and analyzed under fluorescence microscope. The result showed that the knockdown of *HULC* induced apoptosis-related morphological changes, such as nucleus condensation, cell membrane blebbing and cytoplasmic vacuolization compared to control cells (Fig. 3A-C).

Consistent with the results from morphological evaluation, the gene expression data revealed that *HULC* silencing significantly upregulated *Bax* expression at mRNA level in ZR-75-1 ($P=0.001$) and but had no significant effect on MCF-7 and MDA-MB-231. In addition, *HULC* knockdown significantly downregulated *Bcl-2* expression at mRNA level in ZR-75-1 ($P<0.05$), MCF-7 ($P=0.001$) and MDA-MB-231 ($P=0.001$) (Fig. 3D-F).

HULC knockdown can affect cell cycle: To study the growth inhibitory effect of *HULC* knockdown, cell cycle analysis was done using flow cytometry. The percentages of cell population in sub-G1and G1phase in si-NC-transfected ZR-75-1 (as a control) were 0.94 and 77.2 per cent, respectively, and after 72 h transfection

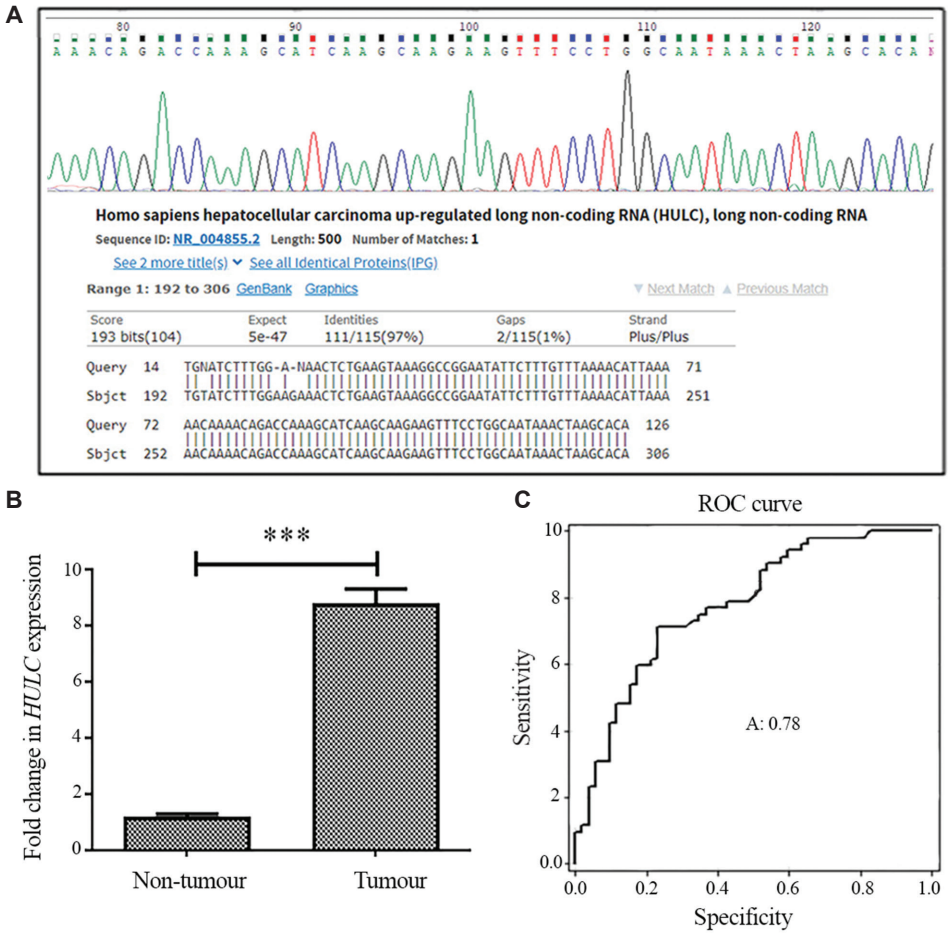

Fig. 1. Expression of *HULC* in breast cancer and receive operating characteristic (ROC) curve analysis for predicting breast cancer prognosis. (**A**) Confirmation of *HULC* expression by Sanger sequencing. (**B**) Real-time qRT-PCR analysis of *HULC* expression level in cancerous and adjacent non-tumour breast tissues. Values are mean±SEM (n=3). (**C**) ROC curve for *HULC* to discriminate between tumour and non-tumour tissues. The area under the ROC (AUC) is 0.78 (P<0.001). The sensitivity and specificity were 0.71 and 0.77, respectively and cut-off value was 17.1. Real-time qRT-PCR, real-time quantitative reverse transcription polymerase chain reaction.

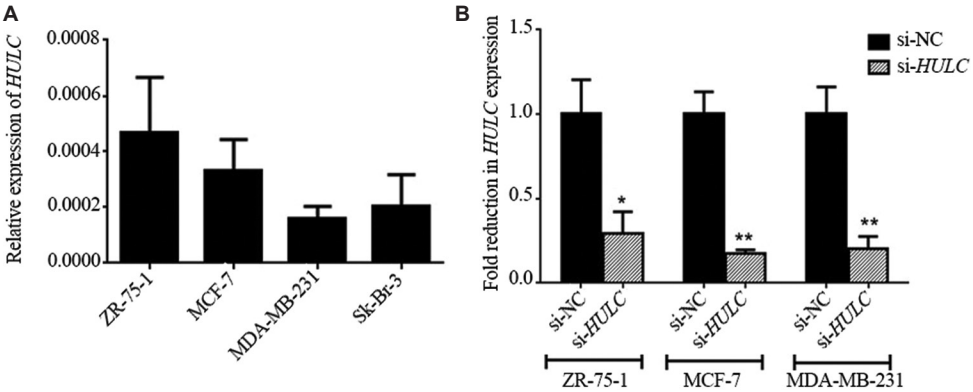

Fig. 2. *HULC* expression in breast cancer cell lines and small interfering (si) RNA -mediated knockdown. (**A**) *HULC* expression levels in breast cancer cell lines including ZR-75-1, MCF-7, MDA-MB-231 and Sk-Br-3. (**B**) The efficiency of si RNA-mediated knockdown was evaluated 72 h after transfection by real-time qRT-PCR in the cell lines. P^{*}<0.05, **<0.01 compared to si-NC. si-NC, small interfering RNA negative control.

Table II. Relationship between highly upregulated in liver cancer expression (HULC) levels and clinicopathological features of patients with breast cancer (n=52)

Characteristics	Number of patients (%)	HULC mean (ΔCt)±SEM	*P*
Age (yr)			
<45	24 (46.7)	15.46±0.75	0.537
>45	28 (53.3)	14.86±0.63	
Tumour size (cm)			
<2	24 (46.2)	14.22±0.69	0.182
>2	20 (38.5)	15.68±0.84	
TNM clinical stage			
I	17 (32.7)	17.10±0.66	0.025
II	14 (26.9)	14.45±1.01	
III	14 (26.9)	13.74±0.87	
Lymphatic metastasis			
Absent	17 (32.7)	15.80±0.61	0.052
Present	28 (53.8)	13.66±0.94	
Differentiation			
Poor	5 (9.6)	12.56±1.46	0.284
Moderate	35 (67.3)	15.26±0.58	
Well	5 (9.6)	15.53±2.13	
Progesterone expression (%)			
<30	13 (38.2)	14.91±1.21	0.914
>30	21 (61.8)	15.06±0.77	
Oestrogen expression (%)			
<30	17 (32.7)	16.12±0.79	0.088
>30	17 (32.7)	13.89±0.99	
HER-2 status			
Negative	16 (30.8)	14.93±1.04	0.891
Positive	15 (28.8)	15.13±0.98	
Location			
Right	20 (38.5)	14.81±0.84	0.549
Left	23 (44.2)	15.45±0.68	

HER-2, human epidermal growth factor receptor-2; TNM, tumour, node, and metastasis; SEM, standard error of mean

with si-*HULC* in the mentioned phases were 13.5 and 65.3 per cent, respectively. Cell population percentage in sub-G1 and G1 in si-NC-transfected MCF-7 (as a control) were 2.07 and 83.8 per cent, respectively, and after 72 h transfection with si-*HULC* were 23.5 and 60.8 per cent, respectively. Measured cell population percentage in si-NC-transfected MDA-MB-231 (as a control) in sub-G1 and G1 were 0.68 and 69.1 per cent, respectively, and after 72 h transfection with si-*HULC* in the mentioned phases were reported to be 15.4 and 55.3 per cent, respectively. Thus, there was a significant reduction in G1 phase in the studied cell lines ($P<0.05$), while the cell percentage in the sub-G1, representing apoptotic cells, was significantly increased following 72 h of *HULC* depletion ($P<0.05$) (Fig. 4).

HULC silencing affects epithelial-mesenchymal transition (EMT): To investigate the role of *HULC* in cell migration and EMT, the invasive behaviour of MCF-7, MDA-MB-231 and ZR-75-1cells was studied following *HULC* attenuation using wound-healing assay. The expression of invasive genes was studied by real-time qRT-PCR. As shown in

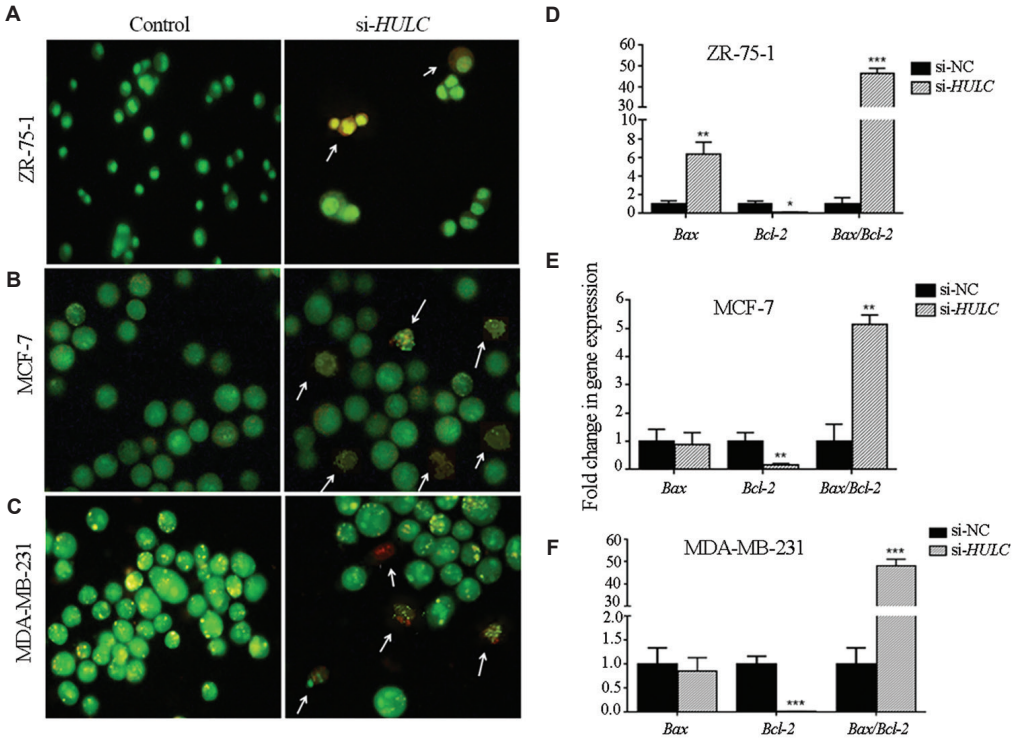

Fig. 3. Effects of *HULC* knockdown on apoptosis. (**A-C**) Morphological evaluation of the apoptotic cells stained with acridine orange/ethidium bromide. Arrows indicate apoptotic cells. Magnification, ×200. (**D-F**) Expression of *Bax* and *Bcl-2* in ZR-75-1, MCF-7 and MDA-MB-231 by real-time qRT-PCR after *HULC* knockdown. Values are mean±SEM (n=3). $P^{*}<0.05$, $^{**}<0.01$, $^{***}<0.001$ compared to si-NC.

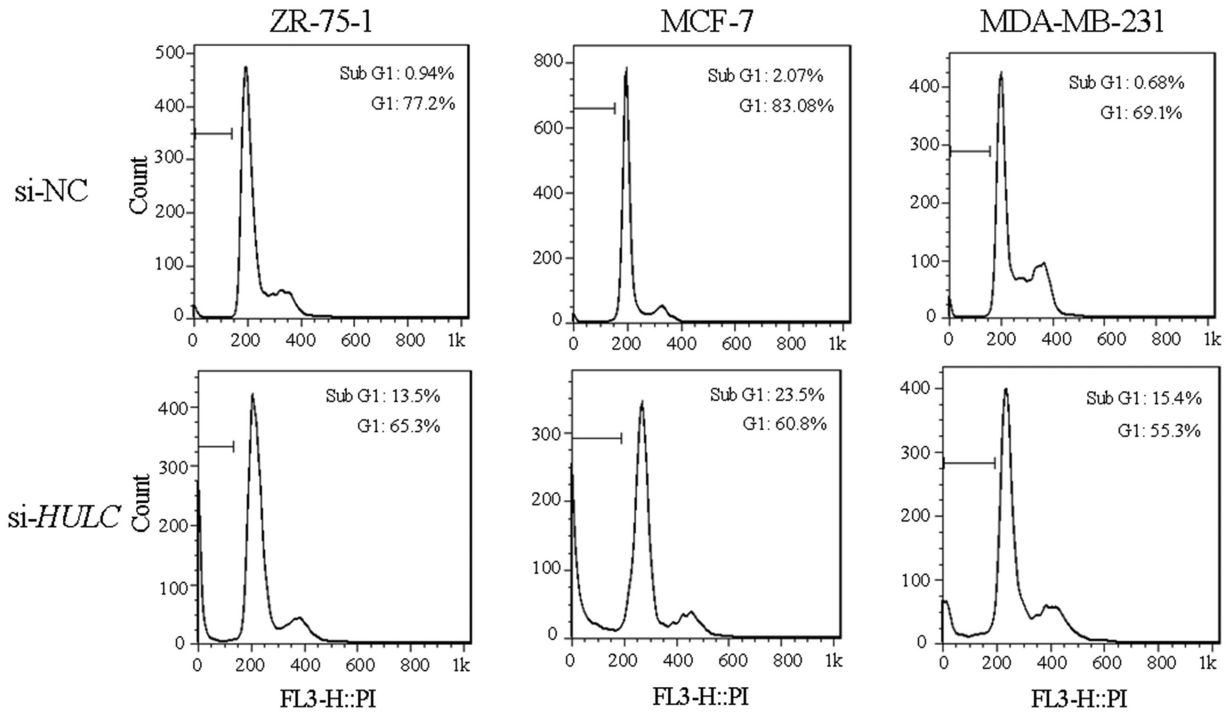

Fig. 4. Cell cycle analysis. ZR-75-1, MCF-7 and MDA-MB-23 cells were transfected with si-NC and si-*HULC*. Propidium iodide (PI) staining was done 72 h after transfection. The range gate illustrated on FACS plots indicates sub-G1.

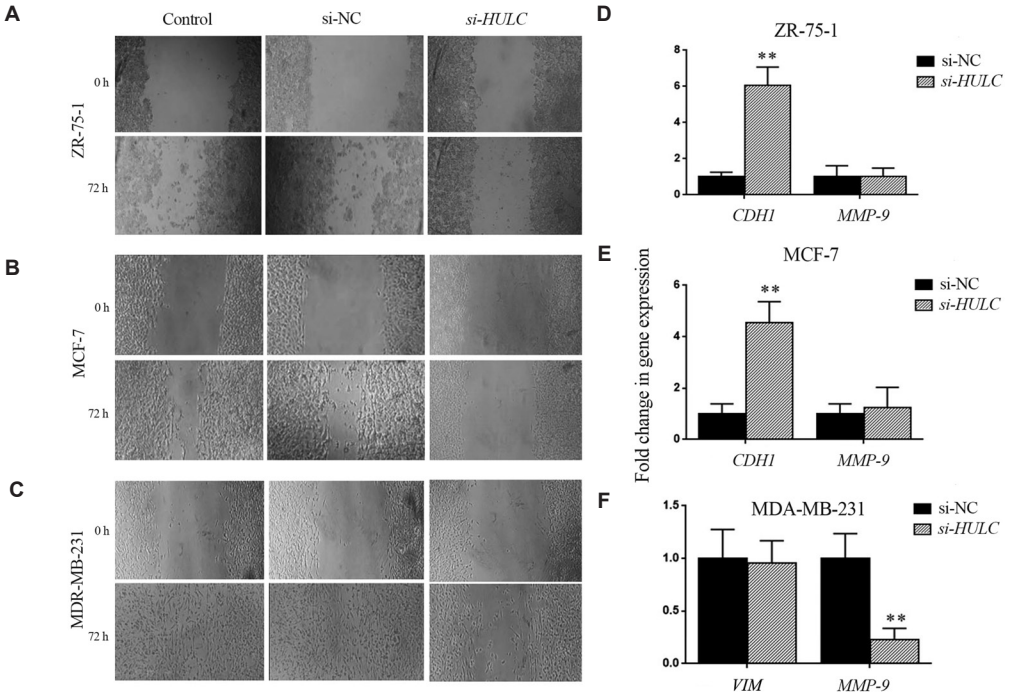

Fig. 5. Effects of *HULC* knockdown on epithelial-mesenchymal transition. (**A-C**) Scratch wound healing assay was performed in control and small interfering RNA -treated breast cancer cell lines ZR-75-1, MCF-7 and MDA-MB-231. Magnification, ×100. (**D-F**) Analysis of *CDH1*, *VIM* and *MMP-9* expression in breast cancer cell lines by real-time qRT-PCR after *HULC* knockdown. Values are mean±SEM (n=3). $^{**}P<0.01$ comapred to si-NC.

Figure 5A-C, knockdown of *HULC* significantly decreased cell migration capacity compared to non-transfected parental cells or si-NC-treated cells ($P<0.05$). Consistent with the wound healing assay results, depletion of *HULC* significantly upregulated E-cadherin in ZR-75-1 cells ($P<0.01$) and MCF-7 cells ($P=0.01$), while vimentin had no significant change in MDA-MB-231. The knockdown of *HULC* downregulated *MMP-9* expression in MDA-MB-231 ($P<0.01$) and had no significant effect on ZR-75-1 and MCF-7 (Fig. 5D-F).

Discussion

In view of the crucial roles of a new class of ncRNAs named lncRNAs in cancer development[20,21], and high incidence of breast cancer among women worldwide[1], the present study was performed to examine the expression levels of lncRNA *HULC* as well as its cellular role in breast cancer. In concordance with earlier studies[7,15,22], our results demonstrated upregulation of *HULC* in breast tumour tissues compared to adjacent non-tumour tissues. Our results revealed the elevated expression levels of *HULC* in advanced clinical stages compared to tumours with early stages. In accordance with the previous studies carried out by Panzitt *et al*[15] and Yang *et al*[17] in HCC and gastric cancer, respectively, our results also showed the biomarker potential of *HULC* in breast cancer.

Inducing apoptosis is an important tool in controlling tumour development. Emerging evidence has demonstrated that increased *Bax*/*Bcl-2* ratio as a hallmark of apoptosis, upregulates caspase-3 and increases apoptosis[23-25]. In 2017, Wang and colleagues[22] reported that *HULC* conspicuously inhibited apoptosis through increase in *Bcl-2* expression levels. Another study performed by Chen *et al*[26] revealed that *HULC* silencing affected apoptosis through upregulation of *Bax* gene. Our findings showed a relationship between *HULC* depletion and apoptosis mostly through reduction in *Bcl-2* and an increase in the ratio of *Bax* to *Bcl-2* expression in breast cancer cell lines. Moreover, apoptosis was further confirmed through increased sub-G1 area in cell cycle analysis.

Cancer metastasis as a major cause of cancer mortality begins with acquiring EMT and invasive properties causing the spread of metastatic cells from primary tumour to different sites[27]. The loss of E-cadherin (epithelial marker) as one of the critical steps in EMT and invasion[28,29] has been considered by many researchers. Li *et al*[30] speculated that lncRNA *HULC* could influence cell migration and invasion

through *HULC*-EMT pathway. Zhao *et al*[7] discovered for the first time that *HULC* was a positive regulator of EMT. They showed that *HULC* depletion induced a repertoire of biochemical and morphological changes causing EMT suppression. In consistent with these findings, our results showed that *HULC* depletion could decrease migration of breast cancer cells and also supress EMT through an increase in the expression of *CDH1*. Upregulation of MMP-9, one of the most widely investigated MMPs, has been reported to play a significant role in different cancers[31]. In this study, a significant reduction of MMP-9 expression was shown in only MDA-MB-231 cells following *HULC* knockdown. Since MMP-9 is highly expressed in triple-negative tumours and is associated with a tumorigenic expression profile and plays critical roles in the metastatic behaviour of MDA-MB-231 cells[32]; we suppose that *HULC* silencing can probably downregulate MMP-9 only in this cell lines.

In this study, *HULC* silencing resulted in a significantly lower expression of *Bcl-2* and higher expression of *CDH1* in breast cancer cells. Our results were consistent with a proposed mechanism in which the upregulation of *Bcl-2* led to loss of *CDH1* and decreased *CDH1*-mediated cell-cell adhesion as well as invasion[33,34]. Thus, based on our results, one possibility for upregulation of *Bcl-2* and loss of *CDH1* might be due to the role of *HULC* in apoptosis *via* modulating *Bcl-2* expression, which in turn results in the regulation of *CDH1* levels[33,34]. However, the concrete mechanisms of how *HULC* regulates genes implicated in metastasis and apoptosis remain to be explored in the future.

To summarize, our findings suggest that *HULC* can be a potential molecular marker for breast cancer and may provide further evidence of its vital role in the biology of cancer. This study also provides preliminary data on the importance of this lncRNA as a possible target therapy against breast cancer.

***Financial support & sponsorship*:** Authors acknowledge the Iranian National Science Foundation (grant no. 93045001), Iran, for financial support.

***Conflicts of Interest*:** None.

References

1. Smith RA, Andrews KS, Brooks D, Fedewa SA, Manassaram-Baptiste D, Saslow D, *et al*. Cancer screening in the United States, 2017: A review of current American Cancer Society guidelines and current issues in cancer screening. *CA Cancer J Clin* 2017; *67* : 100-21.
2. Jagtap SV. Evaluation of CD4+ T-cells and CD8+ T-cells in triple-negative invasive breast cancer. *Indian J Pathol Microbiol* 2018; *61* : 477-8.
3. Esteller M. Non-coding RNAs in human disease. *Nat Rev Genet* 2011; *12* : 861-74.
4. Gibb EA, Brown CJ, Lam WL. The functional role of long non-coding RNA in human carcinomas. *Mol Cancer* 2011; *10* : 38.
5. Peng W, Wang Z, Fan H. LncRNA NEAT1 impacts cell proliferation and apoptosis of colorectal cancer via regulation of Akt signaling. *Pathol Oncol Res* 2017; *23* : 651-6.
6. Liu Y, Sun Z, Zhu J, Xiao B, Dong J, Li X. LncRNA-TCONS_00034812 in cell proliferation and apoptosis of pulmonary artery smooth muscle cells and its mechanism. *J Cell Physiol* 2018; *233* : 4801-14.
7. Zhao Y, Guo Q, Chen J, Hu J, Wang S, Sun Y. Role of long non-coding RNA HULC in cell proliferation, apoptosis and tumor metastasis of gastric cancer: A clinical and *in vitro* investigation. *Oncol Rep* 2014; *31* : 358-64.
8. Brockdorff N. Noncoding RNA and polycomb recruitment. *RNA* 2013; *19* : 429-42.
9. Gao Y, Chen G, Zeng Y, Zeng J, Lin M, Liu X, *et al*. Invasion and metastasis-related long noncoding RNA expression profiles in hepatocellular carcinoma. *Tumour Biol* 2015; *36* : 7409-22.
10. Cui M, Xiao Z, Wang Y, Zheng M, Song T, Cai X, *et al*. Long noncoding RNA HULC modulates abnormal lipid metabolism in hepatoma cells through an miR-9-mediated RXRA signaling pathway. *Cancer Res* 2015; *75* : 846-57.
11. Yan H, Tian R, Zhang M, Wu J, Ding M, He J. High expression of long noncoding RNA HULC is a poor predictor of prognosis and regulates cell proliferation in glioma. *Onco Targets Ther* 2017; *10* : 113-20.
12. Sun XH, Yang LB, Geng XL, Wang R, Zhang ZC. Increased expression of lncRNA HULC indicates a poor prognosis and promotes cell metastasis in osteosarcoma. *Int J Clin Exp Pathol* 2015; *8* : 2994-3000.
13. Qiu M, Xu Y, Wang J, Zhang E, Sun M, Zheng Y, *et al*. A novel lncRNA, LUADT1, promotes lung adenocarcinoma proliferation via the epigenetic suppression of p27. *Cell Death Dis* 2015; *6* : e1858.
14. Huang MD, Chen WM, Qi FZ, Xia R, Sun M, Xu TP, *et al*. Long non-coding RNA ANRIL is upregulated in hepatocellular carcinoma and regulates cell proliferation by epigenetic silencing of KLF2. *J Hematol Oncol* 2015; *8* : 57.
15. Panzitt K, Tschernatsch MM, Guelly C, Moustafa T, Stradner M, Strohmaier HM, *et al*. Characterization of HULC, a novel gene with striking up-regulation in hepatocellular carcinoma, as noncoding RNA. *Gastroenterology* 2007; *132* : 330-42.
16. Peng W, Gao W, Feng J. Long noncoding RNA HULC is a novel biomarker of poor prognosis in patients with pancreatic cancer. *Med Oncol* 2014; *31* : 346.
17. Yang Z, Lu Y, Xu Q, Tang B, Park CK, Chen X. HULC and H19 played different roles in overall and disease-free survival from hepatocellular carcinoma after curative hepatectomy: A preliminary analysis from gene expression omnibus. *Dis Markers* 2015; *2015* : 191029.

18. Lee SB, Sohn G, Kim J, Chung IY, Lee JW, Kim HJ, *et al*. A retrospective prognostic evaluation analysis using the 8th edition of the American Joint Committee on Cancer staging system for breast cancer. *Breast Cancer Res Treat* 2018; *169* : 257-66.
19. Rao X, Huang X, Zhou Z, Lin X. An improvement of the 2ˆ(-delta delta CT) method for quantitative real-time polymerase chain reaction data analysis. *Biostat Bioinforma Biomath* 2013; *3* : 71-85.
20. Nana-Sinkam SP, Croce CM. Non-coding RNAs in cancer initiation and progression and as novel biomarkers. *Mol Oncol* 2011; *5* : 483-91.
21. Yang G, Lu X, Yuan L. LncRNA: A link between RNA and cancer. *Biochim Biophys Acta* 2014; *1839* : 1097-109.
22. Wang J, Ma W, Liu Y. Long non-coding RNA HULC promotes bladder cancer cells proliferation but inhibits apoptosis via regulation of ZIC2 and PI3K/AKT signaling pathway. *Cancer Biomark* 2017; *20* : 425-34.
23. Kulsoom B, Shamsi TS, Afsar NA, Memon Z, Ahmed N, Hasnain SN. Bax, Bcl-2, and Bax/Bcl-2 as prognostic markers in acute myeloid leukemia: Are we ready for Bcl-2-directed therapy? *Cancer Manag Res* 2018; *10* : 403-16.
24. Sharifi S, Barar J, Hejazi MS, Samadi N. Roles of the Bcl-2/Bax ratio, caspase-8 and 9 in resistance of breast cancer cells to paclitaxel. *Asian Pac J Cancer Prev* 2014; *15* : 8617-22.
25. Salakou S, Kardamakis D, Tsamandas AC, Zolota V, Apostolakis E, Tzelepi V, *et al*. Increased Bax/Bcl-2 ratio up-regulates caspase-3 and increases apoptosis in the thymus of patients with myasthenia gravis. *In Vivo* 2007; *21* : 123-32.
26. Chen C, Wang K, Wang Q, Wang X. LncRNA HULC mediates radioresistance via autophagy in prostate cancer cells. *Braz J Med Biol Res* 2018; *51* : e7080.
27. Guan X. Cancer metastases: Challenges and opportunities. *Acta Pharm Sin B* 2015; *5* : 402-18.
28. Myong NH. Loss of *CDH1* and Acquisition of *VIM* in epithelial-mesenchymal transition are noble indicators of uterine cervix cancer progression. *Korean J Pathol* 2012; *46* : 341-8.
29. Murai T, Yamada S, Fuchs BC, Fujii T, Nakayama G, Sugimoto H, *et al*. Epithelial-to-mesenchymal transition predicts prognosis in clinical gastric cancer. *J Surg Oncol* 2014; *109* : 684-9.
30. Li SP, Xu HX, Yu Y, He JD, Wang Z, Xu YJ, *et al*. LncRNA HULC enhances epithelial-mesenchymal transition to promote tumorigenesis and metastasis of hepatocellular carcinoma via the miR-200a-3p/ZEB1 signaling pathway. *Oncotarget* 2016; *7* : 42431-46.
31. Alizadeh AM, Shiri S, Farsinejad S. Metastasis review: From bench to bedside. *Tumour Biol* 2014; *35* : 8483-523.
32. Mehner C, Hockla A, Miller E, Ran S, Radisky DC, Radisky ES. Tumor cell-produced matrix metalloproteinase 9 (MMP-9) drives malignant progression and metastasis of basal-like triple negative breast cancer. *Oncotarget* 2014; *5* : 2736-49.
33. Li L, Backer J, Wong AS, Schwanke EL, Stewart BG, Pasdar M. *Bcl-2* expression decreases cadherin-mediated cell-cell adhesion. *J Cell Sci* 2003; *116* : 3687-700.
34. Karch I, Schipper E, Christgen H, Kreipe H, Lehmann U, Christgen M. Is upregulation of BCL2 a determinant of tumor development driven by inactivation of CDH1/E-cadherin? *PLoS One* 2013; *8* : e73062.

For correspondence: Dr Esmaeil Babaei, Department of Animal Biology, School of Natural Sciences, University of Tabriz, Tabriz 51666, Iran
e-mail: babaei@tabrizu.ac.ir